Application of DTI Visualization and Analysis on a Data Set from a Brain Tumor Patient

Song Zhang David H. Laidlaw* Mark E. Bastin Saurabh Sinha† Thomas S. Deisboeck‡

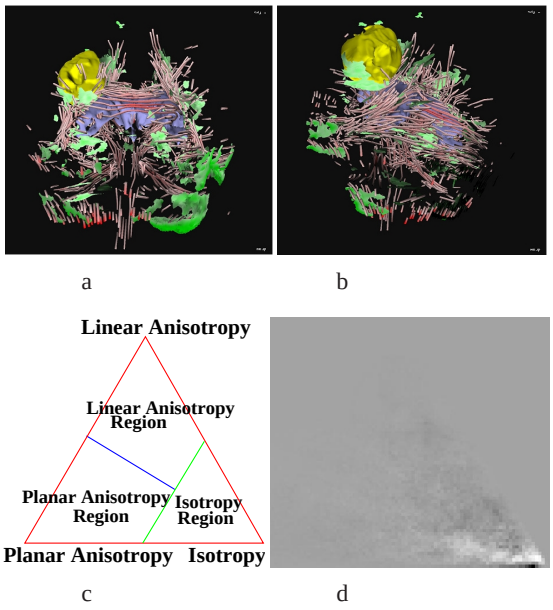

Figure 1: (a,b) Geometric models for visualizing the diffusion anisotropy of water in the brain. Streamtubes and streamsurfaces visualize the diffusion information in linear and planar anisotropic regions respectively. The blue and yellow shapes are isosurfaces of the ventricles and the peritumoral edema. (c) A division of barycentric space into three kinds of anisotropy regions. We generate anisotropy histograms over the barycentric space, and use the division for comparison. (d) The difference of anisotropy histograms over tumor and non-tumor sides of the brain. The brighter area reflects more tumor bearing side data points. The dark region on the top right part of the triangle implies a decrease of linear diffusion anisotropy on the tumor side of the brain. The bright region on the bottom right part implies an increase of planar diffusion anisotropy on the same side. Most of the data points are around the isotropy corner, so we zoom in the picture of the histogram toward that corner.

We demonstrate that 3D reconstruction and visualization can help uncover intriguing features and patterns in a diffusion tensor MR imaging (DTI) data set of a patient suffering from a metastatic brain tumor. We found that the area surrounding both the tumor and its edema is characterized by marked heterogeneity in both linear and planar diffusion anisotropy of water. In fact, similar heterogeneity can be detected throughout the entire brain. Displaying this qualitative diffusion anisotropy information using our 3D immersive virtual reality platform both allow the observer a flexible spatial orientation and enable useful interactive combinations with conventional 2D MRI-sections [1]. Furthermore, by defining the linear and planar diffusion anisotropy regions on the anisotropy domain we were able to show quantitatively that there is an increase in planar anisotropy as well as a decrease in linear anisotropy on the tumor bearing side of the brain.

*Brown University; {sz,dhl}@cs.brown.edu
†University of Edinburgh; {meb,SS}@skull.dcn.ed.ac.uk
‡Massachusetts Institute of Technology and Massachusetts General Hospital, Harvard Medical School; deisboec@helix.mgh.harvard.edu

1 Methods

In December 2001, the 72-year old male patient presented with left facial seizures, left facial weakness, and slurred speech. CT as well as structural and diffusion tensor MR imaging was performed, and the patient was started on corticosteroid therapy (dexamethasone, 16 mg/day). A craniotomy with excision of the brain tumor followed. Histological evaluation confirmed a metastasis from an adenocarcinoma of the lung.

We visualized the DTI data set by generating geometric models that correlate with the underlying structures of the biological tissues. First, we distinguished between regions of linear and planar diffusion anisotropy of water in the DTI data set, and then we employed streamtubes (red) and streamsurfaces (green), respectively, to visualize these two types of anisotropic diffusion (see Figure 1 (a,b)).

The Cave is an $8 \times 8 \times 8$ foot cube with rear-projected front and side walls and a front projected floor. The graphics system can display the virtual environment so that it appears stationary to the user moving through it. We display geometric models of streamtubes, streamsurfaces, ventricles, and the peritumoral edema in the Cave. Two-dimensional T2-weighted MR sections are also displayed to facilitate the anatomical orientation for the user and their current section and axis can be chosen interactively using a viewing wand.

Streamtubes and streamsurfaces visualize diffusion anisotropy qualitatively. However, we also wanted to measure the diffusion anisotropy quantitatively . In Westin's metric [2], diffusion anisotropy is classified as linear anisotropy (cl), planar anisotropy (cp), or isotropy (cs). The three diffusion anisotropy metrics are normalized so that $cl + cp + cs = 1$. Thus, a two-dimensional barycentric space can be used for the domain of all the diffusion anisotropies, where the three anisotropy metrics are used for the barycentric coordinates [3]. We calculated the histogram of a DTI (or a region of a DTI) over this barycentric space while using the T2-weighted image to filter out the data points that were located outside the brain. Figure 1 (c,d) shows the definition of a barycentric space and the difference between the histograms of tumor side and non-tumor side of the brain.

2 Results

Likely having originated at the gray-white matter junction of the brain, the growing metastasis inevitably impacts the structures in the white matter of the brain, thus affecting the anisotropy of water measured by DTI. Comparing both hemispheres, the following regions of linear and planar diffusion anisotropy can be qualitatively distinguished:

1. The T2 peritumoral edema volume is to a certain extent surrounded by planar diffusion anisotropy, which is not present at the

same site on the contralateral, left side. The lack of planar diffusion anisotropy towards the skull corresponds with the proximity of the tumor to the surface of the brain. The medial planar diffusion anisotropy along the longitudinal tracts has a different angle as compared to the contralateral, healthy hemisphere. The planar diffusion anisotropy at the level of the posterior horn of the ventricle, ipsilateral to the tumor, is markedly reduced.

2. Indicated by an increase in red coloring, it appears that there is an increase in linear diffusion anisotropy in some distinct paths, e.g. across the corpus callosum towards the contralateral hemisphere (Figure 1 (a)). A similar phenomenon can be found ipsilateral to the tumor, along the longitudinal tracts posteriorly (Figure 1 (b)).

3. There is a noticeable loss of planar diffusion anisotropy around the cerebellum, ipsilateral to the tumor. Conversely, it appears that there is an increase in linear diffusion anisotropy within the area of the cerebellum, primarily ipsilateral to the tumor, towards caudal (Figure 1 (a)).

The quantitative results of the diffusion anisotropy histogram are listed in Table 1. The expansive tumor and its increasing edema volume, respectively, reduce the total linear diffusion anisotropy ipsilateral to the tumor, and increase the total planar diffusion anisotropy on the tumor side of the brain.

	Left	Right(w/metastasis)
linear anisotropy voxels	36,141	26,667
planar anisotropy voxels	63,317	68,677
% of *linear* anisotropy voxels	12. 2%	17. 1%
% of *planar* anisotropy voxels	31. 5%	30. 0%

Table 1: The results of the diffusion anisotropy histogram are listed for the left as well as for the tumor bearing right side of the brain. We place the green line in Figure 1 (a) at the position that has isotropy value 0. 1.

3 Acknowledgments

This work was supported in part by grant CA69246 from the National Institutes of Health, by the Human Brain Project (NIDA and NIMH), by grants from the National Science Foundation (CCR-0086065, CCR-0093238, and EIA-9724347) and by funds from the Cunningham Trust & William Ramsay Henderson Trust Scholarship (S.S). Imaging was carried out at the SHEFC Brain Imaging Centre, University of Edinburgh, UK. The authors would like to thank especially Dr. E. Antonio Chiocca (MGH-Neurosurgical Service, Harvard Medical School) and Professor Ian Whittle (Department of Clinical Neurosciences, Western General Hospital, University of Edinburgh, UK) for inspiring discussions. Thanks also go to Çağatay Demiralp for help develop the CAVE application.

References

[1] Zhang S., Demiralp C., Keefe D.F., DaSilva M.J., Laidlaw D. H., Greenberg B.D., Basser P.J., Pierpaoli C., Chiocca E.A., and Deisboeck T.S. "An immersive virtual environment for DT-MRI volume visualization applications: a case study." In *IEEE Visualization,* 2001.

[2] Westin C.F., Peled S., Gubjartsson H., Kikinis R., and Jolesz F.A. "Geometrical diffusion measures for MRI from tensor basis analysis." In *Proceedings of ISMRM,* 1997.

[3] Kindlmann G.L., and Weinstein D.M. "Hue-balls and lit-tensors for direct volume rendering of diffusion tensor fields." In *IEEE Visualization 99,* 183-190, 1999.

Application of DTI Visualization and Analysis on a Data Set from a Brain Tumor Patient

S. Zhang, D.H. Laidlaw
Brown University

M.E Bastin, S. Sinha
University of Edinburgh

T.S. Deisboeck
Mass. General Hospital

1. Introduction

We chose a patient suffering from a solitary brain metastasis from a primary lung cancer as an example case for demonstrating the potential of 3D visualization and analysis of DT-MRI data. The geometric models generated from DTI data set provide physicians with useful information about a brain tumor and the peritumoral brain brain. The histograms of anisotropy values in the brain quantify the structural changes caused by the tumor. The combined visualization and computational methods have the potential to assist in preoperative surgery planning as well as postoperative treatment evaluation.

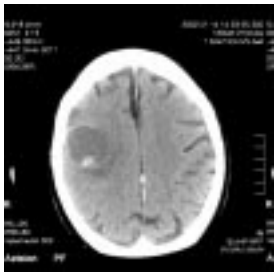

2. Geometric models

We visualized the DT-MRI data by generating geometric models that correlate with the underlying structures of the biological tissues. First, we distinguished between regions of linear and planar diffusion anisotropy of water in the DT-MRI data set, and then we employed streamtubes (red) and streamsurfaces (green), respectively, to visualize these two types of anisotropic diffusion [2,3].
A virtual environment is set up in the CAVE. We display geometric models of streamtubes, streamsurfaces, ventricles, and the tumor inside the data boundary. Two-dimensional T2-weighted MR sections are also displayed to facilitate the anatomical orientation for the user and their current section and axis can be chosen interactively using a viewing wand [3].

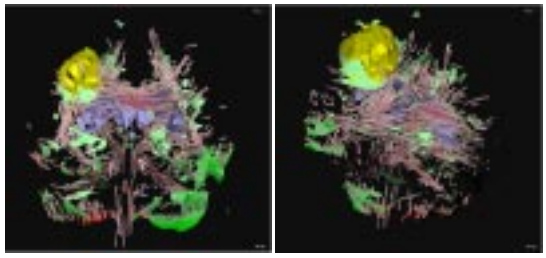

3. Histogram over Barycentric Space

In order to measure the diffusion anisotropy quantitatively, we use a two-dimensional barycentric space for the domain of all the diffusion anisotropies, and calculate the histogram of a DTI region over this barycentric space.
In Westin's metric, diffusion anisotropy is classified as linear anisotropy (cl), planar anisotropy (cp), or isotropy (cs) [4]. The three diffusion anisotropy metrics are normalized so that cl +cp+cs = 1. Thus, a two-dimensional barycentric space can be used for the domain of all the diffusion anisotropies, where the three anisotropy metrics are used for the barycentric coordinates. We calculated the histogram of a DTI (or a region of a DTI) over this barycentric space [5].

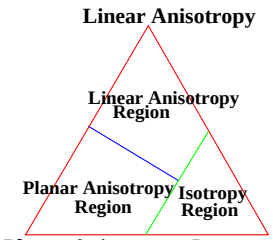

a. We divide the barycentric space into three kinds of anisotropy regions

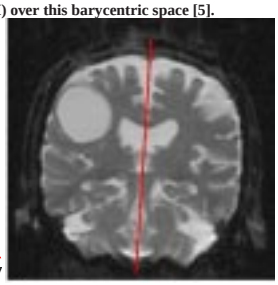

b. A line divides the brain into two regions for comparison

c. Histogram over tumor side of the brain

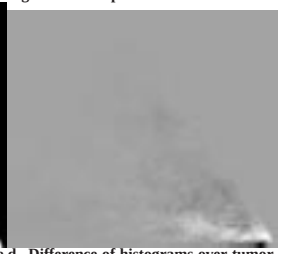

d. Difference of histograms over tumor and non-tumor sides

4. Qualitative Findings

- The tumor volume is to a certain extend surrounded by planar diffusion anisotropy.
- The amount of planar diffusion anisotropy of the corresponding site on the left hemisphere is substantially less and fails to show a similar shell-like pattern as on the tumor bearing side.
- The planar diffusion anisotropy at the level of the posterior horn of the non-tumor side ventricle is markedly reduced.
- Indicated by an increase in red coloring, it appears that there is an increase in linear diffusion anisotropy across the corpus callosum towards the contralateral hemisphere.
- There is a noticeable loss of planar diffusion anisotropy around the cerebellum on the non-tumor side. Conversely, it appears that there is an increase in linear diffusion anisotropy within the area of the cerebellum, primarily on the non-tumor side, towards caudal.

5. Quantitative Findings

The quantitative results of the diffusion anisotropy histogram are listed in Table 1. The expansive tumor and its increasing edema volume, respectively, reduce the total linear diffusion anisotropy ipsilateral to the tumor and increase the total planar diffusion anisotropy on the tumor side.

	Normal side	Tumor side
Linear anisotropy voxels	36,141	26,667
Planar anisotropy voxels	63,317	68,677
% of linear anisotropy voxels	12.2%	17.1%
% of planar anisotropy voxels	31.5%	30.0%

[1] Basser P.J., Pajevic S., Pierpaoli C., Duda J., Aldroubi A., Magn. Res. in Med., 44:625-632, 2000. [2] Zhang S., and Laidlaw D.H., Proc. Int'l Soc. Magn. Reson. in Med., 2001. [3] Zhang S., Demiralp C., Keefe D., DaSilva M., Greenberg B., Basser P., Pierpaoli C., Chiocca E., Deisboeck T., Laidlaw D., Vis. 2001. [4] Westin C.-F., Peled S., Gubjartsson H., Kikinis R., and Jolesz F.A., Proc. Int'l Soc. Magn. Reson. in Med., 1997. [5] Kindlmann G.L., and Weinstein D.M., Vis. 1999

Acknowledgments

This work was supported in part by grant CA69246 from the National Institutes of Health, by the Human Brain Project (NIDA and NIMH), by grants from the National Science Foundation (CCR-0086065, CCR-0093238, and EIA-9724347) and by funds from the Cunningham Trust & William Ramsay Henderson Trust Scholarship (S.S). Imaging was carried out at the SHEFC Brain Imaging Centre, University of Edinburgh, UK. The authors would like to thank especially Dr. E. Antonio Chiocca (MGH-Neurosurgical Service, Harvard Medical School) and Professor Ian Whittle (De-partment of Clinical Neurosciences, Western General Hospital, University of Edinburgh, UK) for inspiring discussions. Thanks also go to Çağatay Demiralp for help develop the CAVE application.